

DUOX Enzyme Activity Promotes AKT Signalling in Prostate Cancer Cells

CHRISTOPHER A. PETTIGREW, JOHN S. CLERKIN and THOMAS G. COTTER

Tumour Biology Laboratory, BioSciences Institute, University College Cork, Cork, Ireland

Abstract. *Reactive oxygen species (ROS) and oxidative stress are related to tumour progression, and high levels of ROS have been observed in prostate tumours compared to normal prostate. ROS can positively influence AKT signalling and thereby promote cell survival. The aim of this project was to establish whether the ROS generated in prostate cancer cells positively regulate AKT signalling and enable resistance to apoptotic stimuli. In PC3 cells, dual oxidase (DUOX) enzymes actively generate ROS, which inactivate phosphatases, thereby maintaining AKT phosphorylation. Inhibition of DUOX by diphenylene iodium (DPI), intracellular calcium chelation and small-interfering RNA (siRNA) resulted in lower ROS levels, lower AKT and glycogen synthase kinase 3 β (GSK3 β) phosphorylation, as well as reduced cell viability and increased susceptibility to apoptosis stimulating fragment (FAS) induced apoptosis. This report shows that ROS levels in PC3 cells are constitutively maintained by DUOX enzymes, and these ROS positively regulate AKT signalling through inactivating phosphatases, leading to increased resistance to apoptosis.*

It is now well-established that reactive oxygen species (ROS) and associated oxidative stress are related to tumour progression. Elevated levels of ROS have been observed in many types of cancer, including prostate cancer, and have been linked to increased tumour aggressiveness, proliferation and metastatic capacity (1). Inherent prolonged oxidative stress in cancer cells can also affect genetic stability and cell survival (2). Intracellular ROS can be generated by NADPH oxidase (NOX) enzymes, and the NOX family contains seven members [NOX1-5, and dual oxidases (DUOX) 1 and 2] which transfer electrons across membranes to molecular

oxygen, producing ROS (3). NOX1-4 require the cytochrome b-245 light chain (p22PHOX) co-factor for full enzyme activity (4, 5), however, NOX5 and the DUOXs do not require a co-factor. Their activity is responsive to changes in intracellular calcium levels, as they contain calcium-binding EF-hand motifs (6, 7). NOX expression is often de-regulated during tumourigenesis and higher than normal tissue, and promotes tumourigenic activity (8-10).

Intracellular ROS have a number of functional roles, as they oxidise lipids, proteins, carbohydrates and nucleic acids. In addition to host defence, ROS can modulate cell signalling pathways by oxidising exposed sulfhydryl groups in the catalytic pockets of protein tyrosine phosphatases (3). While moderate amounts of ROS can positively regulate survival signalling proteins such as AKT (11), excessive ROS generation within a cell can trigger death due to damage to DNA, proteins, lipids or even activation of p38 mitogen-activated protein kinase (MAPK) and extracellular signal-related kinase (ERK) 1 and 2 (3). AKT serine/threonine protein kinases play a crucial role in controlling the balance between cell survival and apoptosis. Apoptosis regulators modulated by AKT include caspase-9, Bcl2-associated death promoter (BAD), and glycogen synthase kinase 3 β (GSK3 β), and phosphorylation of these proteins reduces susceptibility to apoptotic stress (12). Activation of AKT, identified by inducible phosphorylation (Thr308 and Ser473), has been observed in various human malignancies including prostate cancer, and has been linked to tumour progression (13). The present study aimed at identifying the source of ROS in PC3 cells and at determining the role of ROS in maintaining activation of the AKT survival pathway and resistance to apoptotic stimuli.

Materials and Methods

Correspondence to: Professor Thomas G. Cotter, Tumour Biology Laboratory, BioSciences Institute, University College Cork, College Road, Cork, Ireland. Tel: +353214901321, Fax: +353214901382, e-mail: t.cotter@ucc.ie

Key Words: ROS, NOX, apoptosis, survival, peroxide, PC3 cells, prostate cancer, DUOX.

Reagents and antibodies. All reagents were purchased from Sigma-Aldrich (Dublin, Ireland) unless stated otherwise. Antibodies used were NOX2 (GP91PHOX; Upstate, Milton Keynes, UK); NOX4 (a gift from J. David Lambeth, Emory University School of Medicine, Atlanta, GA, USA); DUOX2, phospho-serine (Abcam, Cambridge, UK); Anti-FAS (human-activating clone CH11) (Millipore, Billerica, MA, USA); glyceraldehyde 3-phosphate dehydrogenase

(GAPDH; Advanced Immunochemicals, Long Beach, CA, USA); phospho-tyrosine (Becton Dickinson, Oxford, UK); β -actin and α -tubulin (Sigma-Aldrich, Dublin, Ireland); AKT, phosphorylated AKT (Serine 473), GSK3 β , phosphorylated GSK3 β (serine-9), SRC, phosphorylated SRC (tyrosine 416), phosphorylated SRC (tyrosine-527), BCL2-like 11 (BIM), BAD, phosphorylated BAD (serine-136), phospho-threonine (Cell Signalling Technology, Beverly, MA, USA); NOX1, NOX3, NOX5, DUOX1, p22PHOX, p47PHOX, and p67PHOX (Santa Cruz Biotechnology, Santa Cruz, CA, USA). Rabbit polyclonal antibodies against NOX5 were gifts from W. Nauseef and K-H Krause. Peroxidase-conjugated secondary antibodies were purchased from Dako (Glostrup, Denmark) and fluorescent secondary antibodies were purchased from Li-Cor Biosciences (Cambridge, UK).

Cell culture, flow cytometry and viability assays. PC3 human metastatic prostate carcinoma cells and HeLa human cervical cancer cells were purchased from the American Tissue Type Culture Collection (ATCC; Manassas, VA, USA). PC3 cells were maintained in Kaigh's modified F12 medium (F12-K; Gibco-Invitrogen, Paisley, UK) supplemented with 10% heat-inactivated foetal bovine serum (FBS; Gibco-Invitrogen) and 1% penicillin/streptomycin (Gibco-Invitrogen). HeLa cells were maintained in RPMI1640 supplemented with 10% heat inactivated FBS and 1% penicillin/streptomycin. DU145 and WPMY1 cells (ATCC, Manassas, VA, USA) were maintained in DMEM supplemented with 10% and 5% heat-inactivated FBS respectively, and 1% penicillin/streptomycin. RWPE-1 cells (ATCC, Manassas, VA, USA) were maintained in keratinocyte serum-free media (Gibco-Invitrogen) supplemented with bovine pituitary extract (Gibco-Invitrogen), epidermal growth factor (EGF) (Gibco-Invitrogen) and penicillin/streptomycin. Cells were harvested and resuspended in phosphate buffered saline (PBS) for treatments with the NOX inhibitor diphenylene iodium (DPI; 10-50 μ M), the intracellular calcium chelator 1,2-Bis(2-aminophenoxy)ethane- N,N,N',N' -tetraacetic acid tetrakis(acetoxymethyl ester) (Bapta-AM; 2.5-5 nM), the NOX subunit translocation inhibitor apocynin (1 mM), and the phosphatase inhibitor Calyculin A (10-40 nM; Cell Signalling Technology, Beverly, MA, USA) for 1 h prior to flow cytometry analysis or protein extraction. Rac1 inhibitor (200-800 μ M; NSC23766; Calbiochem/Merck Biosciences, Nottingham, UK) treatment was performed under the same conditions. Small-interfering RNA (siRNA) was transfected into PC3 cells using Lipofectamine RNAiMax (Invitrogen) according to the manufacturer's instructions. siRNAs used were Silencer Select (Ambion, Warrington, UK) pre-designed to DUOX1 (s28797), DUOX2 (s27102) and Negative control (4390844). Cells were harvested for use on the flow cytometer, protein extraction or viability assay after 72 h.

Flow cytometry with 2',7'-dichlorodihydrofluorescein diacetate (H2DCF-DA) conversion to dichlorofluorescein (DCF) and propidium iodide (PI) were performed as previously described (14, 15). Viability assays were performed on PC3 cells transfected with siRNA using the CellTiterBlue Cell Viability Assay kit (Promega, Madison, WI, USA) according to the manufacturer's protocol. For assays involving FAS-ligand death stimulus, the anti-FAS receptor-activating antibody was added to a final concentration of 250 ng/ml per well, 1 h prior to addition of the TiterBlue reagent.

Western blotting and qPCR. Protein extracts were prepared by resuspending cell pellets in ice-cold lysis buffer [50 mM Tris-HCl pH7.4, 150 mM NaCl, 1 mM EGTA, 1 mM Na3VO4, 1 mM NaF,

1% Nonidet P-40, 0.25% sodium deoxycholate, a cocktail of protease inhibitors (Roche Diagnostics, Lewes, UK) and 0.2 mM 4-(2-Aminoethyl) benzenesulfonyl fluoride (AEBSF)] and incubation on ice for 30 min. Debris were removed by centrifugation at 4°C and protein was quantified by the Bio-Rad protein assay (BioRad, Hemel Hempstead, UK). Proteins were resolved using standard denaturing sodium dodecyl sulfate-polyacrylamide gel electrophoresis (SDS-PAGE), followed by transfer to nitrocellulose membranes (Schleicher & Schuell, Whatman, Dassel, Germany). Following blocking and antibody incubations, membranes were either developed using enhanced chemiluminescence agent (Amersham Biosciences, Buckinghamshire, UK) or scanned using the Odyssey® infrared imaging system (Li-Cor Biosciences). Total RNA was extracted using the Trizol reagent (Invitrogen), according to the manufacturer's instructions. cDNA was synthesised using Moloney murine leukemia virus (MMLV) reverse transcriptase (Promega) according to the manufacturer's instructions using oligo dT. Real-time quantitative PCR was performed using Quantitect SYBR Green PCR Master Mix (Qiagen, Crawley, UK) and Quantitect Primer Assays (Qiagen) for p22PHOX (QT00082481) and GAPDH (QT01192646).

Results

Calcium-dependant ROS are associated with the AKT survival pathway in PC3 cells. PC3 cells were measured on a flow cytometer after staining with H2DCFDA to detect for intracellular hydrogen peroxide levels (Figure 1A). PC3 cells were treated with DPI, a flavoenzyme inhibitor of the NOX family of enzymes, at a range of concentrations for 1 h prior to the addition of H2DCFDA. A significant reduction in DCF fluorescence was observed compared to untreated PC3 cells (Figure 1A and B). Addition of 10 μ M DPI resulted in a 29.28% decrease in median DCF fluorescence, while 50 μ M DPI treatment resulted in a decrease of 53.59%, indicating that NOX enzymes are, at least in part, responsible for generating ROS in PC3 cells. AKT signalling was examined by western blotting, and DPI treatment reduced the levels of phosphorylated AKT (serine 473), with no change in the total AKT levels (Figure 1C). The decrease in active AKT corresponded to a decrease in phosphorylated GSK3 β (serine 9) levels, with no change in the levels of total GSK3 β (Figure 1C). Proteins involved in apoptosis were also examined, with pro-apoptotic BIM being found to increase in treatments with low concentrations of DPI, a pattern also observed for phosphorylated BAD (Figure 1C). These results suggest that the ROS generated by NOX enzymes are involved in maintaining AKT phosphorylation and signalling. PC3 cells were then subjected to FAS activation, in the presence or absence of DPI, and the ability of the cells to resist the induction of apoptosis was measured. Cells treated with both DPI and FAS-activating antibody showed a ~5-fold increase in cell death, as measured by PI, when compared to those treated with the activating antibody-alone. This result suggests that in PC3 cells, NOX enzymes generate ROS which contribute to maintaining the AKT survival pathway and resistance to apoptotic stimuli in PC3 cells.

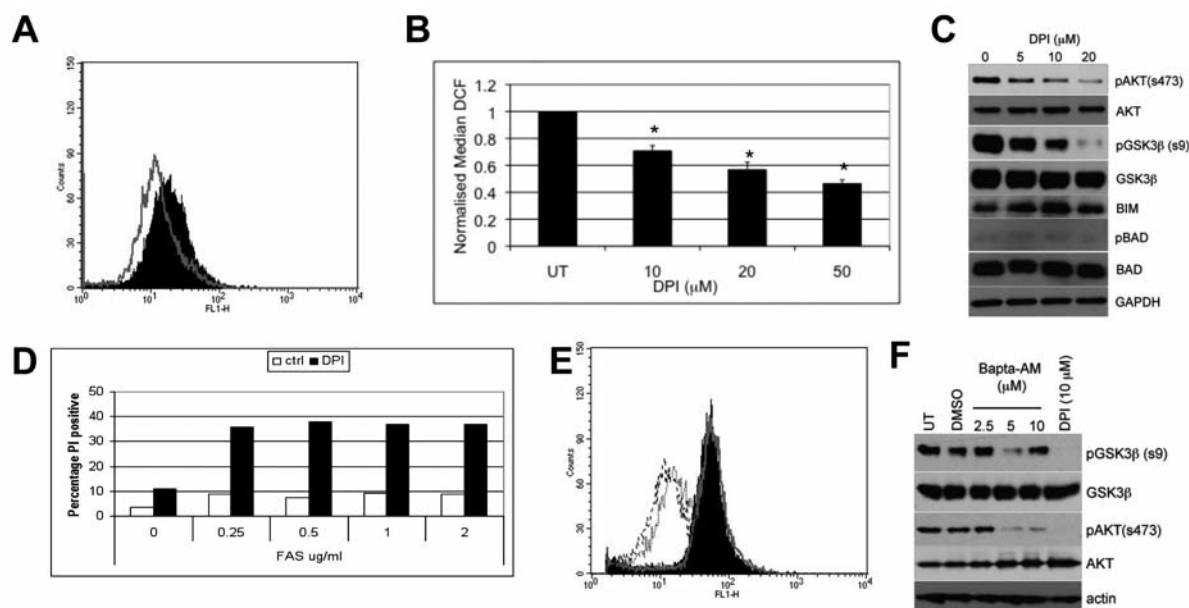


Figure 1. Reactive oxygen species (ROS) generated in PC3 cells can be inhibited by diphenylene iodium (DPI) and increase susceptibility to apoptosis. A: PC3 cells incubated with 2',7'-dichlorodihydrofluorescein diacetate (H₂DCFDA) prior to reading fluorescence on flow cytometer (solid black) or after 1 h of 10 μ M DPI treatment (grey). B: ROS generation with increasing DPI doses (10-50 μ M), as measured by flow cytometry. Asterisks denote $p < 0.005$. C: Western blot analysis of PC3 cells treated with DPI. D: PC3 cell death as measured using propidium iodide (PI) read using a flow cytometer after treatment with apoptosis stimulating fragment ligand (FASL) with and without DPI (10 μ M). E: PC3 cells were incubated with H₂DCFDA prior to reading fluorescence using a flow cytometer (solid black), cells treated with dimethyl sulfoxide (DMSO, vehicle control, grey) and cells treated with 1,2-Bis(2-aminophenoxy)ethane-*N,N,N',N'*-tetraacetic acid tetrakis(acetoxymethyl ester) (Bapta-AM), dotted line (2.5 nM) and dashed line (5 nM). F: Western blot analysis of untreated PC3 cells (UT), treated with DMSO, treated with Bapta-AM and treated with DPI.

In order to determine specifically which member (or members) of the NOX family are responsible for generating the ROS observed in PC3 cells, a number of other compounds that specifically affect NOX activity were used. No change in pAKT was observed with Rac1 inhibitor or apocynin treatment (data not shown). Bapta-AM is an intracellular calcium chelator, and is used to absorb calcium ions within the cell. NOX5 and both DUOX enzymes are responsive to intracellular calcium levels. When treated with 2.5 nM and 5 nM Bapta-AM, PC3 cells displayed a decrease in the levels of ROS, as determined by normalised median DCF fluorescence of 66.32% and 74.75%, respectively (Figure 1E). Protein extracted from PC3 cells treated with increasing concentrations of Bapta-AM showed reduction of phosphorylated AKT (serine 473) and phosphorylated GSK3 β (serine-9) (Figure 1F). These results indicate that the ROS generated in PC3 cells that contribute to AKT survival signalling are calcium ion-dependent, and are likely to come from either one or more of NOX5, DUOX1 or DUOX2.

PC3 cells do not express p22PHOX. Expression of the NOX family of proteins and important enzyme complex subunits in PC3 cells were determined. Expression of NOX1, NOX2,

the NOX4 and NOX5 proteins in PC3 cells were confirmed, while no expression of NOX3 was detected (Figure 2A). DUOX1 and DUOX2 were also detected, as were the subunits p47PHOX and p67PHOX (Figure 2A). p22PHOX was not detected in PC3 cells at either the mRNA or protein level (Figure 2A and B). p22PHOX binds with each of NOX1-4, and these NOX proteins have minimal ROS-generating capability without p22PHOX binding (4, 5). NOX5, DUOX1 and DUOX2 do not rely on p22PHOX for their functional activity. The absence of p22PHOX in PC3 cells reinforces the notion that ROS inhibited by DPI are generated by one or more of NOX5, DUOX1 or DUOX2. In order to determine whether PC3 cells were unique among prostate cell lines in their lack of p22PHOX expression, three other prostate cell lines were examined. DU145 cells are a less tumourigenic prostate cancer cell line, while RWPE-1 and WPMY-1 are considered to be normal prostate lines. Real-time PCR was used to determine the expression levels of *p22PHOX* mRNA across these cell lines. Expression was again undetectable in PC3 cells, however, *p22PHOX* mRNA was found in all other cell lines (Figure 2B). Protein expression levels of p22PHOX were also examined, and expression levels mimicked those observed at the mRNA

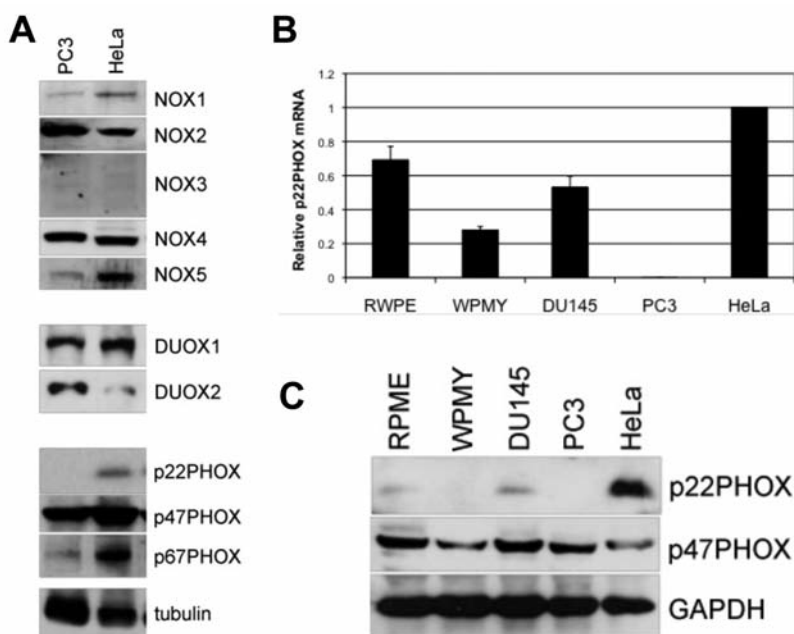


Figure 2. *p22PHOX* is not expressed in PC3 cells. A: Western blot analysis of PC3 and HeLa cell lines for NADPH oxidase (NOX) family proteins. B: Quantitative polymerase chain reaction (Q-PCR) expression data for *p22PHOX* mRNA. C: Western blot analysis for NOX complex subunits.

level (Figure 2C). This result raises the possibility that other NOX enzymes may generate ROS in other prostate cell lines.

DUOX1 and 2 contribute to ROS generation in PC3 cells and AKT phosphorylation. Knockdown of *NOX5* by siRNA in PC3 cells yielded a decrease in ROS levels, but no significant change in GSK3 β phosphorylation or survival was observed (data not shown). siRNA was also used to determine the role of *DUOX1* and *DUOX2* and intracellular ROS in PC3 cells. ROS status was again determined using DCF fluorescence 72 h after transfection and a decrease in ROS was observed with each siRNA. The median DCF fluorescence was reduced by an average of 23.25%, by *DUOX1* siRNA, while a decrease of 18.92% was observed for *DUOX2* siRNA (Figure 3A). This result suggests that both *DUOXs* actively generate ROS in PC3 cells. A modest knockdown of *DUOX1* was confirmed at the protein level by western blot (Figure 3B), with *DUOX1* protein expression reduced to 69.7%. AKT phosphorylation was reduced in *DUOX1* siRNA-treated PC3 cells (37.39%; Figure 3B). GSK3 β phosphorylation was also reduced in *DUOX1* siRNA-treated cells (Figure 3B), suggesting that *DUOX1*-derived ROS may contribute to maintaining phosphorylation of both AKT and GSK3 β . *DUOX2* knockdown was also confirmed at the protein level by western blot (Figure 3C). Phosphorylated AKT was decreased by 47.57% upon *DUOX2* protein knockdown, however there was no change

in the levels of phosphorylated GSK3 β (Figure 3C). Viability assays were also performed on PC3 cells transfected with siRNA against the *DUOXs*, and cell viability was again normalised to that of the negative control siRNA. *DUOX1* siRNA generated a statistically significant decrease of 15.07% in cell viability (Figure 3D) and *DUOX2* siRNA reduced cell viability by 28.45% (Figure 3E). When the transfected PC3 cells were challenged with an antibody activating the FAS receptor, those with *DUOX1* siRNA exhibited a decrease in viability (from 84.93% to 65.73%), indicating an increased susceptibility to apoptosis (Figure 3D). *DUOX2* siRNA-transfected PC3 cells showed no increased susceptibility to FAS-induced apoptosis (Figure 3E). These results suggest that *DUOX1* maintains specific survival signalling in PC3 cells through AKT and GSK3 β , and disruption of this function may increase the susceptibility of these cells to apoptotic stimuli. The *DUOX2* siRNA experiments suggest a role for *DUOX2* in maintaining the viability of PC3 cells, however, this appears to be unrelated to GSK3 β and FAS signalling.

Protein tyrosine phosphatase activity is regulated by NOX-generated ROS in PC3 cells. The AKT survival pathway is negatively regulated by phosphatases and the ROS generated in PC3 cells may inactivate one or more of these phosphatases. PC3 cells were treated with the phosphatase inhibitor calyculin A in the presence and absence of DPI, and

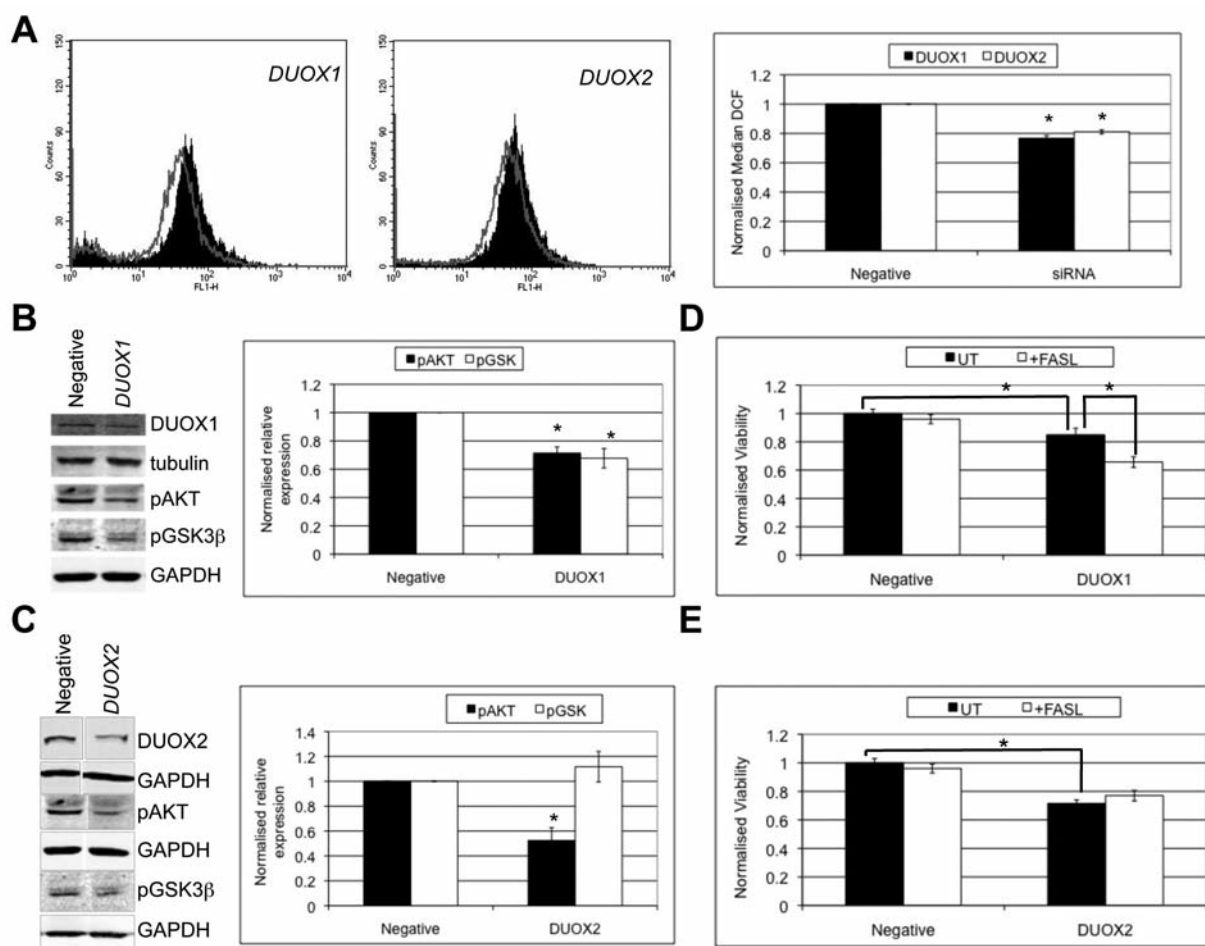


Figure 3. Dual oxidases (DUOX) contribute to reactive oxygen species (ROS) production, AKT and glycogen synthase kinase 3 β (GSK3 β) phosphorylation in PC3 cells and also to cell viability. A: PC3 cells transfected with DUOX1 and DUOX2 siRNA incubated with 2',7'-dichlorodihydrofluorescein diacetate (H₂DCFDA) prior to reading fluorescence on a flow cytometer. Negative control siRNAs are shown in black, DUOX siRNA in grey. A bar chart representation of median DCF fluorescence after siRNA transfection is also shown. Asterisks denote $p < 0.005$. B: Western blot analysis of protein lysate from PC3 cells transfected with DUOX1 siRNA. A bar chart representation of blot quantification is also shown. Asterisks denote $p < 0.005$. C: Western blot analysis of protein lysate from PC3 cells transfected with DUOX2 siRNA. A bar chart representation of blot quantification is also shown. Asterisks denote $p < 0.005$. D and E: PC3 cell viability in the presence or absence of apoptosis stimulating fragment ligand (FASL) and DUOX siRNA as indicated. Asterisks denote $p < 0.05$.

the levels of phosphorylated AKT was examined. Phosphorylation of AKT and GSK3 β remained in samples treated with both DPI and calyculin A (Figure 4A), suggesting that the ROS were no longer effective in the presence of calyculin A in inhibiting phosphatase activity. Calyculin A can inhibit both the catalytic subunit of protein phosphatase-1 (PP1A) and protein phosphatase-2A (PP2A) activity (16), thus it is likely that one of these serine/threonine phosphatases is inactivated by ROS in PC3 cells. Total phosphorylated tyrosine, threonine and serine in PC3 cells treated with DPI were examined by western blot. DPI had no discernible effect on total levels of phosphorylated serine and threonine residues (data not shown), however a reduction in

the amount of total tyrosine phosphorylation was observed (Figure 4B). This result suggests that serine/threonine phosphatases rendered inactive by NOX-derived ROS, maintain AKT phosphorylation, however there is no effect on total serine/threonine phosphorylation levels. Furthermore, NOX-derived ROS act in the cell on one or more protein tyrosine phosphatases. SRC is directly involved in AKT activation. SRC phosphorylation occurs on a number of different tyrosine residues, with phosphorylated tyrosine 416 being a marker of active SRC (17), while phosphorylation at tyrosine 527 is an inhibitory phosphorylation (18). Both of these SRC phosphorylations were reduced in DPI-treated PC3 cells compared to untreated cells (Figure 4C). The reduced

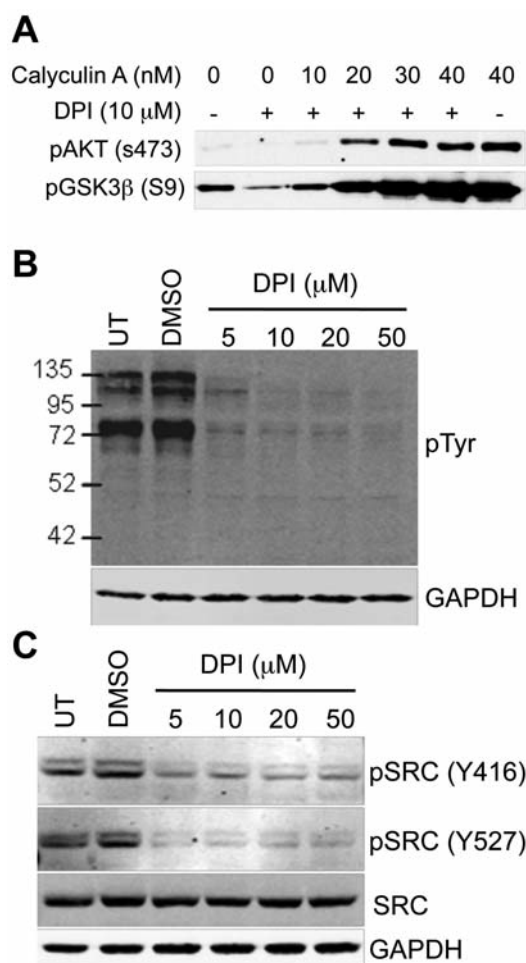


Figure 4. Protein tyrosine phosphatases are inhibited by reactive oxygen species (ROS) in PC3 cells, which maintain AKT phosphorylation. A: Western blot analysis of PC3 cells treated with diphenylene iodium (DPI) and calyculin A. B and C: Western blot analysis of PC3 cells treated with DPI.

amount of active phosphorylated SRC indicates less activity in DPI-treated PC3 cells which may contribute to the observed decrease in AKT phosphorylation.

Discussion

The results presented here show that DUOX1 and DUOX2 are active in PC3 cells, contributing to their basal redox status. PC3 cells are known to have higher levels of endogenous ROS compared to most prostate cell lines (1, 17), and multiple sources of ROS in prostate cancer cells may explain the observation that the NOX inhibitor (DPI) only reduces ROS by up to 46.41% of levels in untreated cells. DPI is also able to inhibit other ROS-generating electron transporters such as nitric oxide synthase, xanthine oxidase,

mitochondrial complex-I and cytochrome *p450* reductase (3). The changes observed in the levels of BIM and phosphorylated BAD at low doses of DPI, suggest that a modest reduction in ROS generation and phosphorylated AKT levels may be sufficient to alter the regulation of anti apoptotic proteins.

Little is known about DUOX activity outside of the thyroid and airway epithelium. Here, we show a modest decrease in ROS levels with knockdown of DUOX1 protein in PC3 cells (Figure 3A). DUOX2 knockdown also reduced ROS levels, as measured by median DCF fluorescence, to a similar level (Figure 3A). As DPI would effectively inhibit both DUOX enzymes in addition to NOX1-5, and NOX5 also generates ROS in PC3 cells (data not shown), the results observed for these proteins, when combined, complement the DPI data. DUOX2 generates ROS in hepatocytes and promotes cell-cycle entry alongside NOX4 in response to platelet-derived growth factor (PDGF) stimulation (19). Knockdown of DUOX2 and NOX4 in these hepatocytes also reduced basal levels of ROS in the absence of stimulation. This complements our observations here in PC3 cells indicating basal NOX5, DUOX1 and DUOX2 activity and maintenance of basal ROS levels.

AKT phosphorylation in PC3 cells is sensitive to changes in ROS levels. While this is indirect, changes of only ~20% in ROS levels can result in a decrease of phosphorylated AKT of ~50% (Figures 1 and 3). While DPI treatment resulted in a decrease in phosphorylated GSK3 β in tandem with AKT (Figure 1C), this was not always observed in the siRNA experiments. GSK3 β can be phosphorylated directly by active AKT, however it can also be phosphorylated by other kinases independently of AKT. In PC3 cells treated with siRNA to *DUOX2*, it appears that GSK3 β phosphorylation is maintained independently of AKT phosphorylation (Figure 3C). AKT is able to confer resistance to resistance to numerous apoptotic stimuli, including FAS ligand (20). An increase in susceptibility to FAS-induced apoptosis was observed in PC3 cells treated with DPI (Figure 1). *DUOX1* siRNA decreased viability (Figure 3D), comparable to the results observed with DPI shown in Figure 1 and *DUOX2* siRNA, while reducing viability to 71.55%, did not sensitize PC3 cells to FAS-mediated apoptosis (Figure 3E). This decrease may arise due to a decrease in proliferation, resulting from DUOX2 no longer up-regulating cyclin-D1 to promote cell-cycle progression (19).

There appears to be a number of oxidative targets affected by ROS, generated by NOX in PC3 cells. PP1A and/or PP2A appear to be oxidised, with calyculin-A blocking dephosphorylation of AKT in the presence of DPI (Figure 4A). However, a decrease in the levels of total tyrosine phosphorylation in PC3 cells was observed in DPI-treated cells (Figure 4B), indicating an increase in protein tyrosine phosphatase activity. SRC is a known target of ROS in other

systems, as SRC activation requires oxidation (18). Active SRC, as determined by phosphorylation on tyrosine 416, was decreased upon treatment with DPI (Figure 4C). While this result may be directly related to that observed with total tyrosine phosphorylation levels, given that SRC is activated by oxidation, it is possible that SRC is activated directly by NOX-derived ROS while activity is also simultaneously being maintained indirectly by NOX-derived ROS. It has previously been shown that SRC can be activated by oxidation in PC3 cells leading to AKT signalling and resistance to anoikis (21), however, those ROS were derived from lipoxygenase. It is possible that SRC activation is maintained in PC3 cells in normal culture through NOX-derived ROS.

The results presented here show that DUOX1 and DUOX2 produce ROS in PC3 cells contributing to basal ROS levels. Furthermore, these ROS are involved in maintaining AKT survival signalling, and resistance to apoptosis. While ROS from each of the NOX enzymes studied here affect AKT phosphorylation, their precise regulation of downstream targets of AKT appears to differ. DUOX1 and DUOX2 appear to contribute to cell viability generally, and DUOX1 may contribute to resistance to apoptosis through AKT signalling. ROS generated by NOX enzymes in PC3 cells may have multiple targets in generating their effects, with PP1A and PP2A implicated in AKT phosphorylation, as well as SRC. The role of NOX enzymes, particularly DUOX1, in survival signalling has yet to be fully determined, but it is clear that PC3 cells use DUOX-derived ROS for maintaining cell viability, suggestive of potential roles for DUOX in prostate tumorigenesis.

Acknowledgements

We thank Dr. Karl-Heinz Krause and Dr. William Nauseef for providing anti-NOX5 antibodies and Dr. J. David Lambeth for providing the anti-NOX4 antibody. This study was supported by Cancer Research Ireland.

References

- Kumar B, Koul S, Khandrika L, Meacham RB and Koul HK: Oxidative stress is inherent in prostate cancer cells and is required for aggressive phenotype. *Cancer Res* 68: 1777-1785, 2008.
- Toyokuni S, Okamoto K, Yodoi J and Hiai H: Persistent oxidative stress in cancer. *FEBS Lett* 358: 1-3, 1995.
- Bedard K and Krause KH: The NOX family of ROS-generating NADPH oxidases: physiology and pathophysiology. *Physiol Rev* 87: 245-313, 2007.
- Kawahara T, Ritsick D, Cheng G and Lambeth JD: Point mutations in the proline-rich region of *p22PHOX* are dominant inhibitors of NOX1- and NOX2-dependent reactive oxygen generation. *J Biol Chem* 280: 31859-31869, 2005.
- Ueno N, Takeya R, Miyano K, Kikuchi H and Sumimoto H: The NADPH oxidase NOX3 constitutively produces superoxide in a p22PHOX-dependent manner: Its regulation by oxidase organizers and activators. *J Biol Chem* 280: 23328-23339, 2005.
- Jagnandan D, Church JE, Banfi B, Stuehr DJ, Marrero MB and Fulton DJ: Novel mechanism of activation of NADPH oxidase 5. Calcium sensitization *via* phosphorylation. *J Biol Chem* 282: 6494-6507, 2007.
- Pacquelet S, Lehmann M, Luxen S, Regazzoni K, Frausto M, Noack D and Knaus UG: Inhibitory action of NOXA1 on dual oxidase activity in airway cells. *J Biol Chem* 283: 24649-24658, 2008.
- Yamaura M, Mitsushita J, Furuta S, Kuniwa Y, Ashida A, Goto Y, Shang WH, Kubodera M, Kato M, Takata M, Saida T and Kamata T: NADPH oxidase 4 contributes to transformation phenotype of melanoma cells by regulating G₂-M cell cycle progression. *Cancer Res* 69: 2647-2654, 2009.
- Fukuyama M, Rokutan K, Sano T, Miyake H, Shimada M and Tashiro S: Overexpression of a novel superoxide-producing enzyme, NADPH oxidase 1, in adenoma and well differentiated adenocarcinoma of the human colon. *Cancer Lett* 221: 97-104, 2005.
- Lim SD, Sun C, Lambeth JD, Marshall F, Amin M, Chung L, Petros JA and Arnold RS: Increased NOX1 and hydrogen peroxide in prostate cancer. *Prostate* 62: 200-207, 2005.
- Naughton R, Quiney C, Turner SD and Cotter TG: BCR-ABL-mediated redox regulation of the PI3K/AKT pathway. *Leukemia* 23: 1432-1440, 2009.
- Manning BD and Cantley LC: AKT/PKB signaling: Navigating downstream. *Cell* 129: 1261-1274, 2007.
- Shukla S, MacLennan GT, Hartman DJ, Fu P, Resnick MI and Gupta S: Activation of PI3K-AKT signaling pathway promotes prostate cancer cell invasion. *Int J Cancer* 121: 1424-1432, 2007.
- Groeger G, Mackey AM, Pettigrew CA, Bhatt L and Cotter TG: Stress-induced activation of NOX contributes to cell survival signalling *via* production of hydrogen peroxide. *J Neurochem* 109: 1544-1554, 2009.
- Mackey AM, Sanvicens N, Groeger G, Doonan F, Wallace D and Cotter TG: Redox survival signalling in retina-derived 661W cells. *Cell Death Differ* 15: 1291-1303, 2008.
- Chatfield K and Eastman A: Inhibitors of protein phosphatases 1 and 2A differentially prevent intrinsic and extrinsic apoptosis pathways. *Biochem Biophys Res Commun* 323: 1313-1320, 2004.
- Giannoni E, Buricchi F, Grimaldi G, Parri M, Cialdai F, Taddei ML, Raugei G, Ramponi G and Chiarugi P: Redox regulation of anoikis: reactive oxygen species as essential mediators of cell survival. *Cell Death Differ* 15: 867-878, 2008.
- Giannoni E, Buricchi F, Raugei G, Ramponi G and Chiarugi P: Intracellular reactive oxygen species activate SRC tyrosine kinase during cell adhesion and anchorage-dependent cell growth. *Mol Cell Biol* 25: 6391-6403, 2005.
- Salmeen A, Park BO and Meyer T: The NADPH oxidases NOX4 and DUOX2 regulate cell cycle entry *via* a p53-dependent pathway. *Oncogene* 29: 4473-4484, 2010.
- Peli J, Schroter M, Rudaz C, Hahne M, Meyer C, Reichmann E and Tschopp J: Oncogenic Ras inhibits FAS ligand-mediated apoptosis by downregulating the expression of FAS. *Embo J* 18: 1824-1831, 1999.
- Giannoni E, Fiaschi T, Ramponi G and Chiarugi P: Redox regulation of anoikis resistance of metastatic prostate cancer cells: key role for SRC and EGFR-mediated pro-survival signals. *Oncogene* 28: 2074-2086, 2009.

Received October 11, 2012

Revised October 30, 2012

Accepted October 31, 2012